Environmental Science & Technology

pubs.acs.org/est

Article

Comparative Metagenomics of the Active Layer and Permafrost from Low-Carbon Soil in the Canadian High Arctic

Xiaofen Wu, Archana Chauhan, Alice C. Layton, Maggie C. Y. Lau Vetter, Brandon T. Stackhouse, Daniel E. Williams, Lyle Whyte, Susan M. Pfiffner, Tullis C. Onstott, and Tatiana A. Vishnivetskaya*

Cite This: *Environ. Sci. Technol.* 2021, 55, 12683−12693

Read Online

ACCESS | Metrics & More | Article Recommendations | Supporting Information

ABSTRACT: Approximately 87% of the Arctic consists of low-organic carbon mineral soil, but knowledge of microbial activity in low-carbon permafrost (PF) and active layer soils remains limited. This study investigated the taxonomic composition and genetic potential of microbial communities at contrasting depths of the active layer (5, 35, and 65 cm below surface, bls) and PF (80 cm bls). We showed microbial communities in PF to be taxonomically and functionally different from those in the active layer. 16S rRNA gene sequence analysis revealed higher biodiversity in the active layer than in PF, and biodiversity decreased significantly with depth. The reconstructed 91 metagenome-assembled genomes showed that PF was dominated by heterotrophic, fermenting Bacteroidota using nitrite as their main electron acceptor. Prevalent microbes identified in the active layer belonged to bacterial taxa, gaining energy via aerobic respiration. Gene abundance in metagenomes revealed enrichment of genes encoding the plant-derived polysaccharide degradation and metabolism of nitrate and sulfate in PF, whereas genes encoding methane/ammonia oxidation, cold-shock protein, and two-component systems were generally more abundant in the active layer, particularly at 5 cm bls. The results of this study deepen our understanding of the low-carbon Arctic soil microbiome and improve prediction of the impacts of thawing PF.

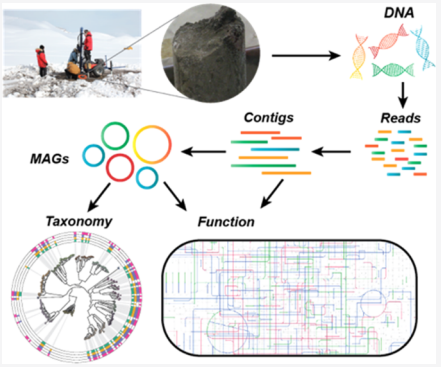

KEYWORDS: *Arctic, permafrost, active layer, 16S rRNA, metagenome-assembled genome, metabolism*

1. INTRODUCTION

Permafrost (PF) regions of the Earth are considered important landscapes that serve as reservoirs for more than half of the estimated global soil organic carbon (SOC).[1] Soils in PF regions consist of two horizons; the active layer (AL), which lies on top, contains soil that undergoes a seasonal freeze−thaw process, and PF, which lies beneath the AL, consists of perennially frozen ground. It is generally accepted that thawing of PF as a result of global climate change will have long-term consequences on the concentration of atmospheric carbon (primarily in the form of CO_2 and CH_4)[2] due to microbial degradation of sequestered carbon. Especially, the potential positive carbon-cycle feedback loops are of concern,[3,4] which may occur when SOC-rich PF regions thaw and become CH_4-emitting wetlands.[5,6] However, SOC-rich PF regions are not the dominant soil type in the Arctic; instead, an estimated 87% of the Arctic consists of SOC-poor mineral PF.[7] Because PF-affected regions encompass a number of different types of plant-dominated biomes[8] as well as SOC and mineral types,[9,10] the impact of geographical and ecological variability on gaseous emission and sequestration needs to be understood better in order to more reliably predict the long-term consequences of climate change.

Biological carbon sequestration in the warming Arctic has been proposed to occur primarily via increased photosynthetic activity and transfer of fixed carbon below ground (i.e., carbon sink).[11] In contrast, natural sources of carbon emission result primarily from respiration, which can be traced back to higher eukaryotes or soil microbes. Multiple physical and biological factors may influence the carbon cycle including soil chemistry, the availability of nutrients such as nitrogen, and the structure of present microbial communities. Recent research suggests that microorganisms play key roles in global fluxes of CO_2, CH_4, and N_2O;[12] however, the response of microbes to PF thawing is considered as an unknown variable.[13] Our understanding of the microbial community structures from PF regions is relatively limited with a disproportionate focus on the microbial communities in relatively high-SOC cryosols such as spruce forests in Alaska[14] or peatlands in Norway[15] rather than more prevalent SOC-poor mineral-rich cryosols.[16] It is well-documented that plants can shape microbial community structures[17] but less is known about microbial community structures in regions with little to no plant growth.

Received: February 3, 2021
Revised: July 27, 2021
Accepted: July 28, 2021
Published: September 2, 2021

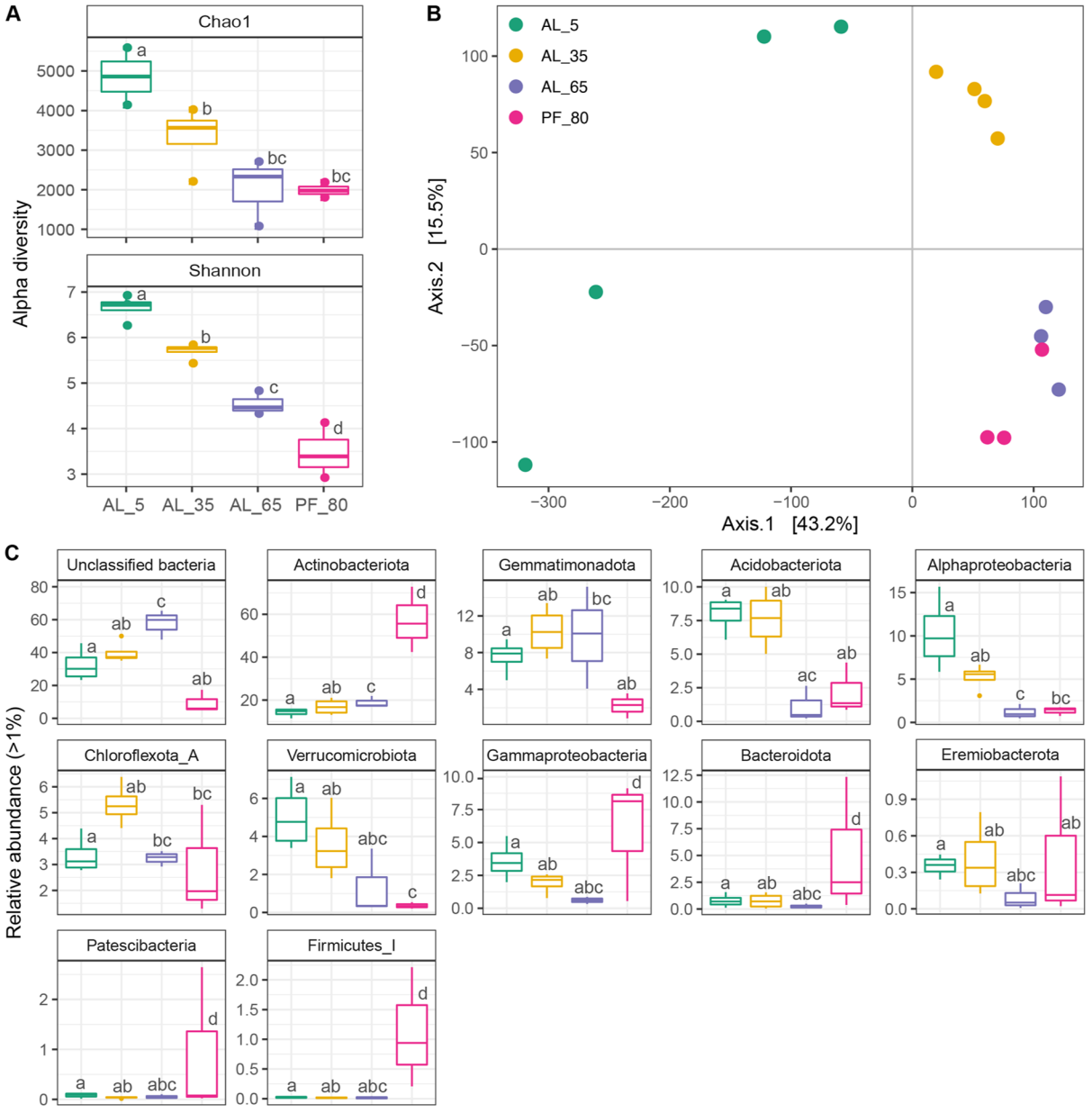

Figure 1. (A) Alpha diversity indexes, (B) principal coordinates analysis of the abundance of microbial communities, and (C) relative abundance of significantly different taxonomy between depths using 16S rRNA gene amplicon sequencing. The letters denote statistical differences between depths. Samples with the same letter are not significantly different. Color codes for the samples are shown as in (B).

Recently, it has been demonstrated that acidic mineral cryosols from the sparsely vegetated Canadian High Arctic sites may serve as a CH_4 sink[18] and a CO_2 source.[19] However, the percentage of microbial sequences recovered from these environments attributable to methanotrophs is low (~1−2%).[18,19] Thus, questions remain as what microbes exist in this sparely vegetated low-carbon biome and what carbon and nitrogen sources they utilize. This study compared the microbial taxa and associated functions in SOC-poor samples of ALs at various depths and PF using 16S ribosomal RNA (rRNA) gene amplicon and metagenome sequencing. The primary goal was to investigate the differences between the phylogenetic profile and the genetic potential of microbial communities in the active and PF layers.

2. MATERIALS AND METHODS

2.1. Site Description, Sampling, and Geochemistry. The McGill Arctic Research Station (MARS) located at Axel Heiberg Island, Nunavut Canada (79°24′54.4″N, 90°44′35.6″W) represents a polar desert environment.[18,19] The SOC content ranged from 1 to 6% in the top 10 cm to <1% below 10 cm,[19] and it was lower than that in the peat and fen sites in Russia (3.6−18.3%)[20] and Alaska (2−20%).[21] Soil cores of 1 m length were collected as previously described,[19] and the details are provided in Supporting Information. The upper 70 cm of the cores represents the AL that was subjected to seasonal thaw, whereas the lower part (>70 cm depth) represents the PF that remained constantly frozen.[19] Four depths (5, 35, 65, and 80 cm samples defined as AL_5, AL_35, AL_65, and PF_80, respectively) were analyzed from each of the four cores, with the exception of PF_80 obtained only from

https://doi.org/10.1021/acs.est.1c00802
Environ. Sci. Technol. 2021, 55, 12683−12693

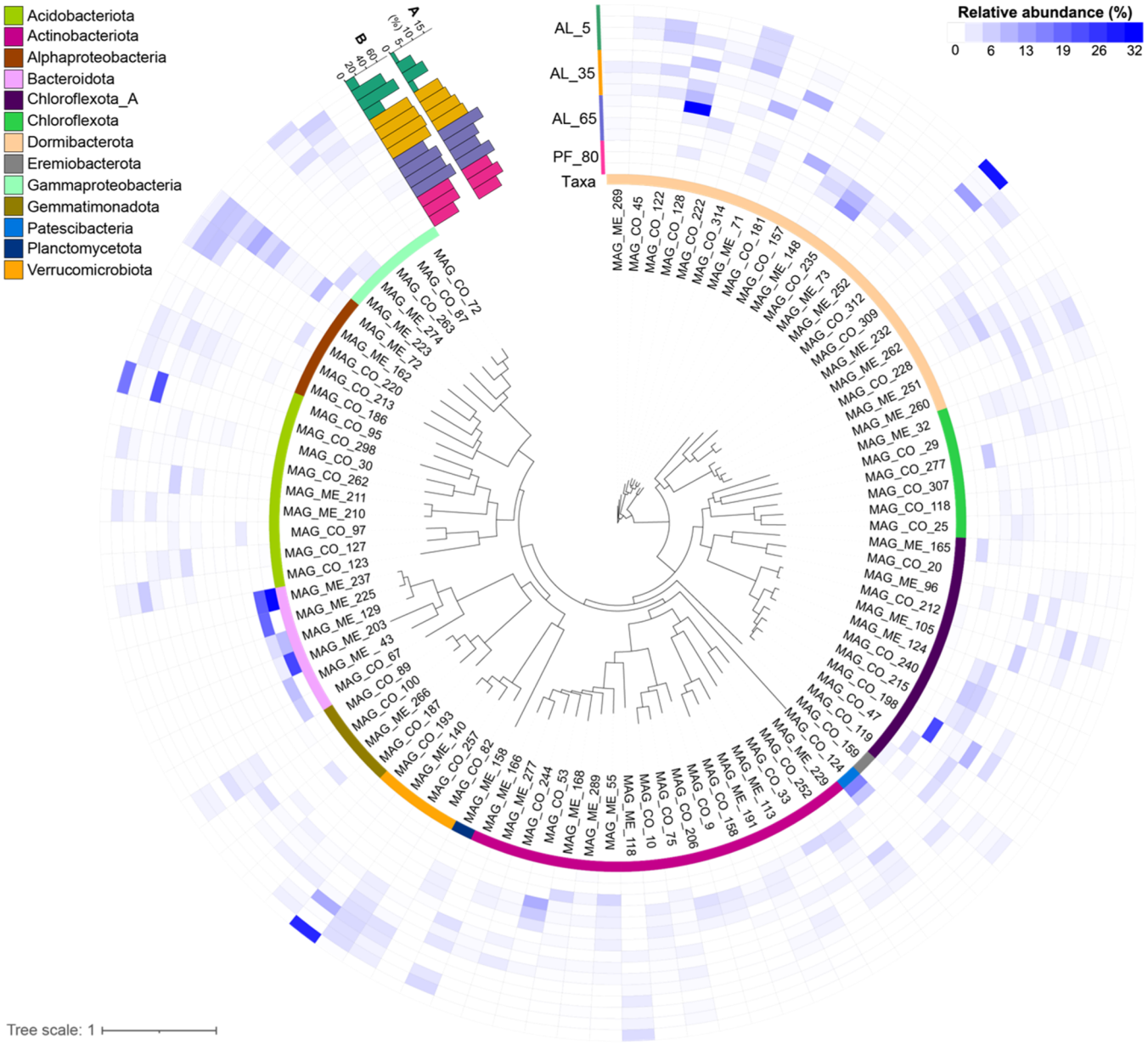

Figure 2. Whole-genome phylogenetic tree and heatmap showing the recovered MAGs and their relative abundance from four depths. The bar plot shows the total percentage of reads mapped to the MAGs (A) and the number of MAGs recovered in the corresponding samples (B).

three cores (Table S1). Chemical characteristics of the soils used in this study were collected when soils started thawing and measured as described in the previous study.[19]

2.2. DNA Extraction, Cell Number Estimation, qPCR, and Sequencing. Total community genomic deoxyribonucleic acid (gDNA) (including both extracellular and intracellular DNA) was extracted using a FastDNA SPIN kit for soil (MP Biomedicals, Irvine, CA).[22] An estimation of cell numbers using fluorescent *in situ* hybridization (FISH) and quantitative polymerase chain reaction (qPCR) analyses for 16S rRNA genes was performed.[22] Both 16S rRNA gene amplicons and metagenomic libraries of community gDNA were sequenced on an Illumina HiSeq 2000 platform. Details of the above listed procedures can be found in Supporting Information.

2.3. Bioinformatics and Statistical Analyses. The 16S rRNA gene amplicon and metagenome sequencing data were processed through established tools and pipelines. The details and statistical analyses are described in Supporting Information.

2.4. Data Availability. Amplicon sequencing data and metagenome raw reads were deposited under NCBI BioProject accession numbers PRJNA694190 and PRJNA261849, respectively (Table S1).

3. RESULTS AND DISCUSSION

3.1. Geochemical Characteristics of the Soils. Geochemical analyses of the samples revealed soils originating from depths of 5, 65, and 80 cm to be slightly acidic with the lowest pH at 80 cm (pH = 5.5) and the highest at 5 cm (pH = 6). No pH measurements were available for 35 cm depth (Table S2). Concentrations of Na, K, Fe, Mg, Si, Ni, and S were significantly higher at 80 cm than at 5 cm ($p < 0.05$). Soils at 35 cm had the highest concentration of *K* compared to other depths ($p < 0.05$). There was no significant difference in

https://doi.org/10.1021/acs.est.1c00802
Environ. Sci. Technol. 2021, 55, 12683−12693

concentrations of Ca, Al, Fe, Sr, Ba, Cr, Cd, Co, Acetate, Br^-, Cl^-, F^-, NO_3^-, PO_4^{3-}, and SO_4^{2-} between depths. Although not deemed significant, principal component analysis (PCA) showed that different compounds exhibited slightly elevated levels at different depths, such as Cl^- at 5 cm, *K* at 35 cm, NO_3^- at 65 cm samples, and SO_4^{2-} at 80 cm depth (Figure S1).

3.2. Estimation of Microbial Cell Numbers. Estimation of total cell numbers (including bacteria, archaea, and eukaryotes) using FISH showed 7.5×10^7 cells g^{-1} in PF. These numbers were lower compared to those in 5 and 65 cm AL samples (1.1×10^8 and 9.5×10^7 cells g^{-1}, respectively) but higher than those at the 35 cm horizon (6.2×10^7 cells g^{-1}, Figure S2). This trend was also true for bacterial cells. Eukaryotic cells decreased from 1.9×10^7 cells g^{-1} at 5 cm to 7.8×10^6 cells g^{-1} at 80 cm, whereas archaea increased from 8.9×10^5 cells g^{-1} at 5 cm to 8.9×10^6 cells g^{-1} at 65 cm while being below the detection level in PF samples. In general, the microbial community was dominated by bacteria, followed by eukaryotes and archaea. As estimated by FISH, bacteria comprised 81.17% of microorganisms in the 5 cm layer and 89.57% in PF, while eukaryotes decreased from 17.98% in 5 cm to 10.43% in PF. The maximum percentage of archaea (9.34%) was observed at 65 cm.

Bacterial cell numbers were also evaluated using qPCR, suggesting a maximum of $\sim 2.9 \times 10^8$ cells g^{-1} soil at 35 cm; assuming an average of 3.6 16S rRNA gene copies per cell,[23] a decreasing trend was seen for 16S rRNA genes with depth (Figure S2). However, for both FISH and qPCR-based assessments of cell numbers, no statistically significant differences were observed between different depths. Discrepancies in bacterial cell counts between the two measurements could be related to biases from environmental properties (pH, metals, etc.), DNA extraction efficiency, yield of nucleic acid, primer specificity, stringency of hybridization, and so forth.[24,25] Thus, the high concentrations of K, Mg, Al, Sr, and Cu in samples collected at 35 cm (Table S2) could bias FISH analysis of microorganisms due to disruption of cell membranes or DNA damage.[26] In the case of qPCR, the results obtained for the 35 cm sample collected at the edge of polygon[19] were ~10 times higher than for samples from the polygon interior.

3.3. Microbial Community from 16S rRNA Gene Amplicon Sequencing and Metagenome Binning. Alpha diversity of the soil samples was highest at 5 cm (Shannon and Chao1, $p < 0.05$) and decreased significantly with depth (Shannon, $p < 0.05$, Figure 1A). Principal coordinate analysis (beta diversity) of all sample's zero-radius operational taxonomic units (OTUs) (zOTUs, analogous to amplicon sequence variants)[27] showed that microbial communities also significantly differed between depths (Figure 1B, PERMANOVA, $p < 0.05$). One exception to this trend was observed in the ice-rich core collected near the rim of the polygon (called edge/ice core).[19] The metagenome from 80 cm PF of this core was closely related to microbial communities from 65 cm (Figure 1B) potentially due to perturbations of sedimentary material along an ice wedge.[28] Similar to the alpha and beta diversity analyses, there was a difference in taxonomic abundance between the active and PF layers, with Actinobacteriota, Gammaproteobacteria, Bacteroidota, Patescibacteria, and Firmicutes_I having a higher relative abundance in PF ($p < 0.05$), whereas a higher abundance of unclassified bacteria, Verrucomicrobiota and Gemmatimonadota was identified in the ALs (Figures 1C and S3). Due to the high abundance of unclassified bacteria observed in the ALs (averaging 32.32−57.73%), in addition to the genome taxonomy database (GTDB), the zOTUs were also annotated using the SILVA rRNA database. Using the latter reference, only 3.83−16.76% of the sequences were assigned to unclassified bacteria, and Chloroflexi was the most abundant taxon in the ALs (Figure S4). This discrepancy was likely caused by the limited number of 16S rRNA genes derived from GTDB as 16S rRNA genes often failed to assemble in metagenome-assembled genomes (MAGs).[29−31] Despite this shortcoming, GTDB is a phylogenetically more consistent, genome-based taxonomy that better reflects evolutionary relationships among microorganisms,[32,33] and was therefore chosen for taxonomic classification of the MAGs recovered in this study. Overall, our data were in line with previous studies, showing that microbial communities in active layers were more diverse and taxonomically different from the underlying PF.[34,35] Despite the dissimilar phylogenetic distribution between the active and PF layers, the majority of taxa were detected at all depths.

A total of 91 MAGs with a completeness ≥70% and contamination ≤10% were reconstructed from the 15 PF metagenomes, altogether contributing 1.45−17.59% of sequencing reads (Figure 2). They spanned 13 bacterial phyla; no MAGs were affiliated with archaea (Figure 2 and Table S3), although archaeal genomes were previously recovered and reported from the same sampling sites.[36] Of the 91 recovered MAGs, 57 MAGs were retrieved from all depths, while Bacteroidota and Patescibacteria MAGs were exclusively detected at 65 and 80 cm. In addition, the single Planctomycetota MAG was only identified at 35, 65, and 80 cm. Relative abundances of individual MAGs did not vary significantly between depths in the AL and PF. Based on the relative abundance of the MAGs, the metagenomic data revealed that the ALs were dominated by MAGs associated with the poorly characterized phylum Dormibacterota (29−38.08% relative abundance of microbes binned into MAGs, Figure 2), in comparison to the low abundance of this phylum detected in the 16S rRNA gene amplicon sequencing analysis (Figure S3). The mismatch abundance of Dormibacterota in the ALs likely related to the fact that MAGs often lack 16S rRNA genes.[29] Phylogenetic analysis showed a predominance of Bacteroidota MAGs in PF (43.18%), suggesting an adaptation of these bacteria to freezing conditions. However, this picture may be skewed as revealed by the conflicting number of unassembled metagenomic reads and co-assembled contigs (data not shown) and in particular by the 16S rRNA gene amplicon sequencing analysis. These methods instead indicated that microbial communities from the PF were dominated by Actinobacteriota (Figures 1C and S3), which represented only 11.74% of the recovered communities. This contrast originated in our disproportionate inability to bin complete or near-complete Actinobacteriota MAGs and underlined the importance of not losing sight of the unbinned data in metagenomic analysis. Finally, differences between the two sequencing methods could have contributed to the phylogenetic differences between the 16S rRNA gene amplicon and metagenome sequencing data as 16S rRNA gene amplicon sequencing can introduce biases from PCR amplification. In general, the microbial community structure identified by both methods was similar to that found in previously studied PF soils[14−16,37] and was consistent with

https://doi.org/10.1021/acs.est.1c00802
Environ. Sci. Technol. 2021, 55, 12683−12693

results, indicating that Proteobacteria, Actinobacteriota, and Acidobacteriota were commonly found across soils of all temperatures and independent of plant association.[38,39] In addition, our data showed that the poorly characterized phyla were present in the studied environments, such as Dormibacterota, Eremiobacterota, and Patescibacteria. These phyla have been shown to be abundant in dry, bare soil environments[40] and have reduced redundant and nonessential functions.[41]

3.4. Metabolic Potential in Active and PF Layers. The reconstructed 91 MAGs were assessed for the presence of specific KEGG orthologies (KOs) associated with hydrolysis, fermentation, electron donor utilization, electron acceptors, ability to fix CO_2 and N_2, motility, bacterial secretion, and stress response (Tables S4−S6). These data were used to identify different suggested potential growth strategies (Figures 4 and 5). All quoted percentage values in the sections below refer to the averages of relative abundance of the MAGs from the replicated metagenomes (see Supporting Information). In addition to the genomic analysis, the whole community gene content present at a certain depth was also analyzed. Discrepancies between this analysis and MAG functional analysis originated from the fact that only a small portion of reads were binned into MAGs (totaling 1.45−17.59% of mapped reads per sample, Figure 2). The purpose of the gene-centric analysis of un-binned metagenomic sequences was to investigate the previously "hidden" portion of reads and to elucidate differences between the two methods. In general, gene abundance in metagenomes of the whole community was consistent with the trends identified by analysis of MAGs. Therefore, the results reported here will be limited to selected key functions or to discussion of instances where the two analyses stand in contradiction. The overall microbial metabolic potential determined by assessing the diversity of all KOs differed significantly between depths (Figure 3, PERMANOVA, $p < 0.05$).

3.4.1. Cellulose Degradation is a Common Feature in PF. Cellulose and xylan, derived from plant cell walls, make up a large proportion of SOC in land ecosystems. Chitin originates from fungi and insects and is another abundant polysaccharide in the terrestrial ecosystem.[42] The breakdown of these polysaccharides results in the release of short oligo/disaccharides which can be further processed to obtain energy (e.g., during glycolysis or fermentation).[42] The complete degradation of cellulose is a multi-step process.[42] Populations that could encode the capacity for the complete degradation of cellulose to glucose, primarily belonging to the Bacteroidota, were particularly abundant at 80 cm (46.91% relative abundance of microbes binned into MAGs, Figures 4 and S5), with significance when compared to 5 cm ($p < 0.05$), suggesting that the potential ability to degrade cellulose was a common feature in PF and thawing is likely to stimulate microbial decomposition and respiration of sequestered carbon.[21] The lowest percentage of microorganisms encoding these genes was identified at 5 cm (4.09%), even though SOC was up to 6% in upper 10 cm in comparison to <1% in lower layers.[19] Microorganisms containing only cellulase genes coding for the potential to convert cellulose to cello-oligosaccharide were identified in 12 MAGs, with the highest abundance at 65 cm (19.10%) and the lowest at 80 cm (3.21%). 22 MAGs showed genes encoding β-glucosidase to degrade cello-oligosaccharides to glucose but lacked cellulase genes for the initial steps in cellulose breakdown. β-Glucosidase encoding populations, primarily represented by Acidobacteriota, was significantly more abundant at 5 cm (36.44%) than at other depths ($p < 0.05$), suggesting that a majority of the recovered communities from 5 cm were opportunistic, taking advantage of cellulase-producing primary degraders.

Initial xylan degradation is carried out by xylanases, while the released xylobiose is further processed to xylose and smaller oligosaccharides by β-xylosidases.[42] Only a small fraction of recovered communities was suggested to carry out the complete degradation of xylan to xylose (0.68−3.18%) with an exception of 24.11% of the PF populations from 80 cm (Figure 4). The overall lower incidence of pathways for complete xylan breakdown suggested that cellulose was the more commonly utilized polysaccharide for the recovered populations. One MAG affiliated with Actinobacteriota contained xylanase genes but lacked β-xylosidases genes and was enriched in the 80 cm PF layer (1.77%). MAG_CO_206 and MAG_ME_43, aligning with Actinobacteriota and Bacteroidota, respectively, which could potentially utilize xylobiose but not xylan, were also identified. A relatively high abundance of these xylobiose scavengers was detected at 80 cm (2.93%) and decreased in more shallow, AL samples (2.40 and 0.05% at 65 and 35 cm, respectively). Approximately 25.36−45.75% of the communities recovered from various depths included genes encoding chitinase (Figure 4). These populations with the potential to degrade chitin were the lowest at 5 cm and the highest at 80 cm. MAGs affiliated with Bacteroidota were the dominating populations of chitinase encoding microorganisms at 80 cm (Figure S5). Previous studies showed that cellulose- and chitin-degradation genes were commonly retrieved from both the AL and PF.[14,16,43] Enrichment of hydrolysis genes, important for degrading cellulose and xylan, in PF was also confirmed by gene-centric analysis in our study. In contrast, chitin degradation was shown in a significantly higher abundance in the ALs by gene abundance analysis ($p < 0.05$, Figure S6), indicating a sequestration of chitin and plant-derived polysaccharide degradation.

3.4.2. Populations Rely on Fermentation in PF. Carbon degradation can occur by respiration and/or fermentation, and many organisms are capable of both processes. Fermentation

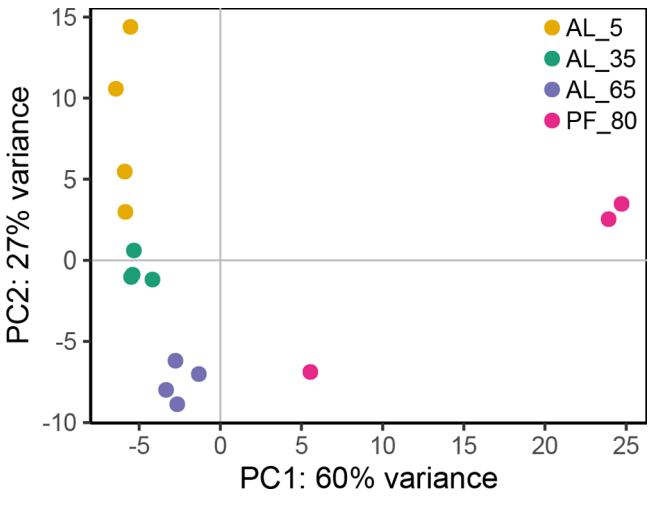

Figure 3. PCA plot visualizing the variation between the samples in the diversity of potential metabolism based on their KO abundances.

https://doi.org/10.1021/acs.est.1c00802
Environ. Sci. Technol. 2021, 55, 12683−12693

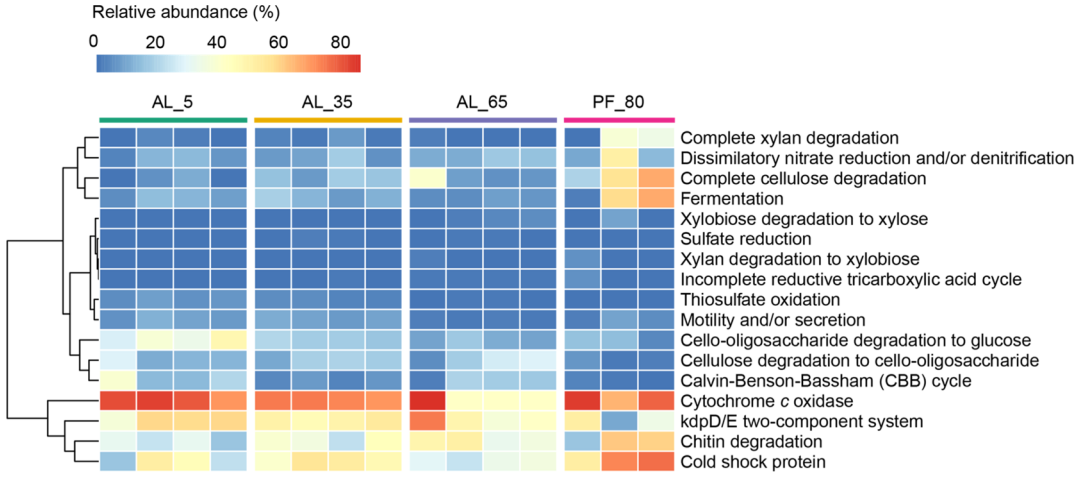

Figure 4. Heatmap showing the total relative abundance of MAGs containing genes coding for the corresponding metabolisms.

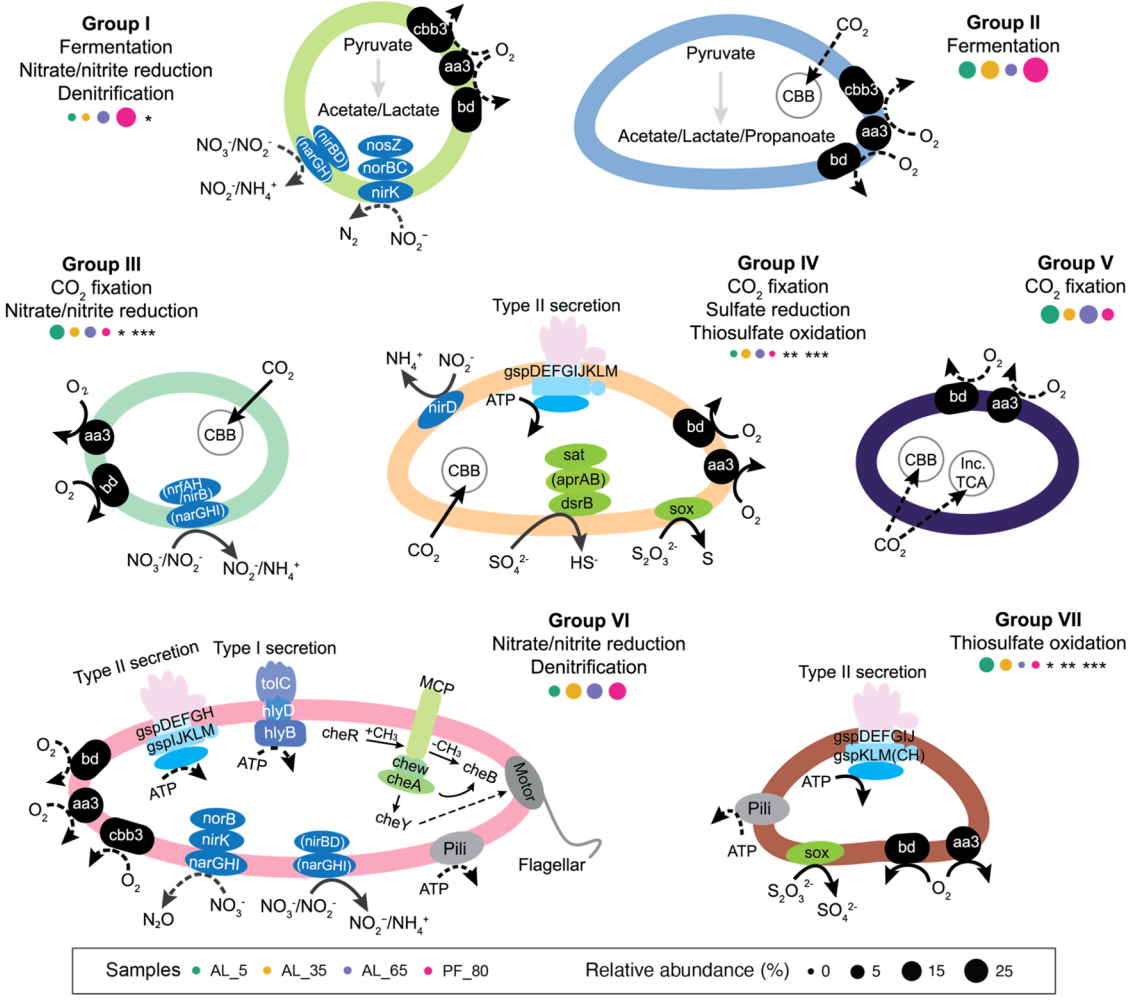

Figure 5. Genome-enabled metabolic potential of different groups which are defined in Table S4. Gene names with brackets and arrows with dashed line indicate that the gene or the pathway was not identified in all the populations within the group. Abbreviations: cbb3, *cbb3*-type cytochrome *c* oxidase; aa3, *aa3*-type cytochrome *c* oxidase; bd, cytochrome *bd* ubiquinol oxidase; CBB, Calvin-Benson-Bassham cycle; and Inc. TCA, incomplete reductive TCA cycle; *$p < 0.05$ between 5 and 80 cm; **$p < 0.05$ between 35 and 80 cm; and ***$p < 0.05$ between 65 and 80 cm.

pathways are a common way for the degradation of monosaccharides and generate adenosine triphosphate, although at lower efficiency, without the use of external electron acceptors. Of the 91 MAGs recovered, 14 contained genes involved in fermentation of pyruvate to acetate, lactate, and/or propanoate (Figure 5 and Table S5). These populations, primarily belonging to Bacteroidota, were particularly abundant at 80 cm (42.09% relative abundance

https://doi.org/10.1021/acs.est.1c00802
Environ. Sci. Technol. 2021, 55, 12683−12693

of microbes binned into MAGs), while only approximately 5.92−12.15% was suggested to have genes coding for pyruvate fermentation in the ALs (Figures 4 and S5). Acetate was the primary fermentation product encoded by Actinobacteriota MAGs at 5 cm, while it was propanoate for Dormibacterota and Actinobacteriota MAGs at 35 and 65 cm, respectively. Fermentation of pyruvate to lactate was found to be more common in PF, primarily conducted by Bacteroidota-aligned MAGs. Overall, our data suggested that fermentation played an important role in anaerobic degradation potential of SOC in PF, which was in line with a previous metagenome study of Alaska PF.[44]

3.4.3. Methane, Nitrogen, and Sulfur Metabolism. Despite no MAGs identified which contained genes encoding CH_4 oxidation in this study, *pmoABC*/*amoABC* genes coding for aerobic CH_4 oxidation were identified at all depths with an overall low abundance within the un-binned metagenome data (0.29−11.74 TPM). The occurrence of these genes was the largest at 5 cm, significantly higher than in PF ($p < 0.05$, Figure S7), suggesting the potential to oxidize a substantial amount of CH_4 and thus potentially limiting the emission of CH_4 into air. This was consistent with a report indicating High Arctic mineral cryosols to potentially serve as CH_4 sinks.[18,45] It should also be noted that these genes are involved in aerobic oxidation of both CH_4 and ammonia, which may explain their higher occurrence in the top layer. In contrast, genes encoding the key enzyme in methanogenesis, methyl-coenzyme M reductase, were not identified in this study. This was in agreement with studies showing that methanogenesis was extremely limited in the AL and PF soil in Alaska and Northern Sweden.[35,46]

N_2 fixation was also not shown to be present in the MAGs, although, the *nifH* gene (KO: K02588) involved in this process was identified at 65 and 80 cm within the un-binned metagenomic data, albeit at very low abundance (0.26 and 0.06 TPM, respectively, $p > 0.05$, Figure S8). Nitrogen fixation genes were found to be highly abundant in the Canadian High Arctic[16] and at the carbon-rich PF site in Alaska;[14] however, the low abundance of the *nifH* gene indicated that the potential for N_2 fixation was limited in the studied environments. 19 MAGs linked organic carbon degradation to dissimilatory nitrate reduction and/or denitrification. Such communities were identified to be most enriched in PF (24.85% relative abundance of microbes binned into MAG), followed by the 65, 35, and 5 cm ALs (13.40, 9.88, and 8.70%, respectively, Figure 4). MAG_ME_223 and MAG_CO_220 identified as similar to *Ramlibacter tataouinensis_A* and Alphaproteobacteria, respectively, showed genes coding for dissimilatory reduction of nitrate to ammonium and were exclusively identified in PF (1.92 and 1.42%, respectively, Figure S5). Furthermore, seven MAGs were suggested to be limited to the reduction of nitrate to nitrite. These populations, most of which represented Actinobacteriota, exhibited their highest abundance at a depth of 65 cm (8.82%, Figure S5). Populations capable of reducing nitrite to ammonium, but not nitrate to nitrite, were identified in nine MAGs. These strains, primarily classified as Bacteroidota, were enriched at 80 cm (15.79%), consistent with the higher concentration of ammonium observed in PF (Table S2). MAG_ME_223 was also suggested to carry out denitrification by converting nitrate to nitrous oxide. A second population was represented by MAG_ME_43 (most related to the Bacteroidia class) that also had the ability to reduce nitrite to nitrogen gas. Although denitrifying bacteria were previously reported to be active in the ALs of this sampling location,[47] these two MAGs capable of near-complete steps of the denitrification process were only identified in PF, representing 4.85% of the recovered communities (Figure S5).

Another potential anaerobic electron acceptor is sulfate that can be converted to sulfide by dissimilatory sulfite reductase. The presence of microbes that use sulfate as a terminal electron receptor in PF has been reported in previous studies.[35,44,48] The Gammaproteobacteria MAG_CO_72 contained one of the key genes (*dsrB*) coding for dissimilarity sulfate reduction and represented a small fraction of the community at 5, 35, and 65 cm (0.09, 0.88, and 0.73%, respectively, Figure 4). The low abundance of sulfate-reducing MAGs presumably illustrated the rarity of this pathway in the studied environments, which was consistent with high levels of sulfate in all layers (Table S2) and was plausible considering the availability of other anoxic electron acceptors with a higher standard reduction potential like nitrate. Thiosulfate oxidation via the conserved *sox* operon (*soxABCDXYZ*) results in the formation of sulfate, whereas the incomplete version (*soxABXYZ*) results in incomplete oxidation of the substrate and leads to either intra-[49,50] or extracellular[51] accumulation of elemental sulfur. Thiosulfate oxidation as a mean to gain energy was identified in three Gammaproteobacteria MAGs, including MAG_CO_72, MAG_CO_87, and MAG_CO_263, with a significantly higher abundance at 5 cm (6.45%) than at other depths ($p < 0.05$, Figure 4). Although both MAG_CO_87 and MAG_CO_263 exhibited the fully conserved *Sox* pathway, MAG_CO_72 was limited to oxidizing thiosulfate to element sulfur. None of the MAGs were suggested to reduce sulfate in PF; however, gene-centric analysis showed that the PF exhibited a generally higher abundance of *dsrAB* (K11180 and K11181) genes encoding sulfate reduction than the ALs but only reached significance compared to 5 cm ($p < 0.05$, Figure S7). Despite the higher presence of potential sulfate-reducing bacteria, PCA indicated an elevated level of sulfate in PF. This may be due to the generally low gene abundance of sulfate reductase (totaling 5.97 TPM).

3.4.4. Cytochrome c Oxidase is Widespread in the Recovered Communities. Despite the broad genetic potential for fermentation and anaerobic respiration across the MAGs, in particular from the PF, genes coding for the key aerobic respiration enzyme cytochrome *c* oxidase were identified in 58 MAGs, with an overall large abundance of the recovered communities from all depths. They were lowest at 65 cm (52.64% relative abundance of microbes binned into MAGs) and highest at 5 cm (77.99%, Figure 4). Genes for aerobic respiration by low-affinity *aa3*-type cytochrome *c* oxidase[52,53] were identified in 42 MAGs. These populations were most abundant at 5 cm (55.34%, Figure S5). A *cbb3*-type cytochrome *c* oxidase was detected at 65 and 80 cm, although with only marginal recovery from 65 cm (0.07 and 43.36%, respectively). This high-oxygen affinity terminal oxidase[52,53] was almost exclusively encoded by Bacteroidota, Alpha-, and Gammaproteobacteria MAGs (totaling seven MAGs) in PF. Genes encoding cytochrome *bd* oxidases, which also exhibit high O_2 affinity,[54] were identified in 37 MAGs and were likewise most enriched at 80 cm (63.67%), although curiously followed by 5, 35, and 65 cm (55.95, 48.20, and 34.65%, respectively). The presence of genes encoding both low- and high-affinity cytochrome oxidase suggested that the recovered

https://doi.org/10.1021/acs.est.1c00802
Environ. Sci. Technol. 2021, 55, 12683−12693

populations were capable of operating under a range of O_2 concentrations. Given the low abundance of fermentation and anaerobic respiration in the ALs, the widely distributed cytochrome *c* oxidase suggested that aerobic respiration was the dominating energy acquisition pathway in the microorganisms present in the ALs, in line with a recent study of Svalbard PF population.[55] Genes encoding the high-O_2 affinity cytochrome *bd* oxidases were also significantly enriched at 5 and 80 cm compared to 35 and 65 cm using gene-centric analysis ($p < 0.05$, Figure S9). The abundance of these genes also appeared to be higher at 5 cm than at 80 cm, albeit not significantly.

3.4.5. Carbon Dioxide Fixation and Biofilm Formation. MAG_ME_168 affiliated with Actinobacteriota contained genes encoding carbon dioxide fixation via the incomplete reductive tricarboxylic acid (TCA) cycle and was most abundant at 80 cm (1.95% relative abundance of microbes binned into MAGs, Figure 4). MAGs containing genes (*cbbL* and/or *cbbS*) encoding ribulose-bisphosphate carboxylase (RubisCO), the key enzyme in CO_2 fixation via the Calvin−Benson−Bassham (CBB) cycle, were identified in this study. Six MAGs, including members of Actinobacteriota, Chloroflexota_A, and Alpha- and Gammaproteobacteria, contained both *cbbL* and *cbbS* genes encoding form I Rubisco, which occurs in photo and chemoautotrophic organisms (Figure S10 and Table S3).[56] Two Dormibacterota MAGs and one Chloroflexota_A MAG only included the *cbbS* gene likely due to incompleteness of the reconstructed genomes (81.76−90.58% completeness). These populations were more abundant in the ALs than in PF, particularly at 5 and 65 cm (21.14 and 13.94%, respectively, $p < 0.05$, Figure 4). One Bacteroidota and Gammaproteobacteria MAG encoded the *cbbL* gene assigned to Rubisco-like proteins (RLPs; form IV), which is incapable of catalyzing RuBP-dependent CO_2 fixation.[57] The function here was unknown; however, several studies indicated that RLPs may be involved in sulfur metabolism, methionine salvage pathway, and D-apiose catabolism.[58,59] These two MAGs were only identified in PF (8.52%), while the Bacteroidota MAG was also found at 65 cm (0.05%, Figure S10 and Table S3). Although the CBB cycle is more energetically demanding compared to other CO_2 fixation pathways,[60] our data suggested that the CBB cycle was the predominant pathway for CO_2 fixation in the recovered populations.

Populations suggested to carry out surface attachment, and/or extracellular polymeric substance secretion were identified. MAG_ME_223 and MAG_CO_87 (both related to Gammaproteobacteria) were suggested to code for type IV pili-assisted motility and type II secretion that could potentially be involved in biofilm formation (Table S6). MAG_CO_72 and MAG_CO_263, likewise closely aligning with Gammaproteobacteria, contained genes encoding type II secretion, while MAG_CO_186 (most related to Alphaproteobacteria) was suggested to have a type I secretion system. MAG_ME_274 closely related to *Methylotenera* sp002429455 contained genes implicated in flagellar and type IV pili-driven motility. Finally, MAG_CO_127, most close to Acidobacteriota, showed genes with the potential for motility via type IV pili. These populations were most abundant at 35 cm (8.86%), significantly higher than at 65 cm (1.66%, $p < 0.05$, Figure 4). Biofilm formation has been suggested to enable microorganisms to have higher resistance against extreme temperature[61] and thus may help these populations to survive under freezing conditions. Under this hypothesis, however, it remains unclear why the 5 cm sample, likely subjected to the harshest temperature fluctuations, does not display a large potential for biofilm formation.

3.4.6. Stress Responses. In order to survive freezing conditions, PF microorganisms were previously suggested to contain genes encoding proteins associated with cold adaptation, such as cold-shock proteins (CSP) and osmotic stress proteins.[62] Genes coding for CSP were identified in 44 MAGs and were significantly more abundant in PF (66.40% relative abundance of microbes binned into MAGs) than at 5 and 65 cm (33.81 and 30.41%, respectively, $p < 0.05$), while approximately 48.54% of the recovered communities contained genes encoding CSP at 35 cm (Figure 4). Although superficially this appears to indicate less cold-adaptation potential in the exposed 5 cm samples, there was in fact a higher abundance of CSP genes detected in the total communities at 5 cm (838 TPM, Figure S9), demonstrating that a large proportion of uncovered populations at 5 cm was adapted to the cold conditions. In contrast, Hultman *et al.*[35] found high numbers of CSPs in PF in comparison to the AL and bog soils in Alaska.

Two-component systems (TCSs) are ubiquitous in nature and are part of regulatory system sensing and responding to alterations in environmental conditions, such as pH, osmolarity, or nutrient availability.[63−65] The populations recovered in this study were enriched in genes for TCSs involved in regulation of potassium (*kdpD/E*)[66] and phosphate transport (*phoR/B*),[67] coping with osmotic stress (*envZ/ompR*)[68] and maintaining membrane fluidity (*desR/K*, Table S6).[69] 46 MAGs contained genes encoding *kdpD/E* TCS which is involved in regulating K^+ homeostasis and appears to play a critical role in challenging environments.[66] The abundance of these populations was highest at 5 cm (53.05%) and lowest at 80 cm (31.85%, Figure 4), suggesting *kdpD/E* was an important regulatory system in response to K^+ limitation and osmotic stress in particular for populations recovered from the ALs. It is conceivable that this was due to the frequent occurrence of meltwater and coinciding changes in ion concentrations. Dominant contributors to the *kdpD/E* expression potential were Acidobacteriota at 5 cm, Dormibacterota at 35 and 65 cm, and Actinobacteriota at 80 cm (Figure S5). Genes coding for other TCSs, such as cell fate and cell cycle control, were also identified in a low number of MAGs. Within the un-binned metagenome data, the AL at 5 cm had a significantly higher abundance in the total TCS potential than at 65 and 80 cm (the sum of normalized abundances of all TCS-related KOs per sample, $p < 0.05$, Figure S9). The occurrence of total TCSs was also higher at 5 cm than at 35 cm, albeit not significantly. The overall high abundance of genes encoding CSP and TCSs in the ALs revealed distinctive characteristics of the community, which must cope with extreme seasonal temperature shifts including repetitive freezing in order to survive.

The genome-centric metagenome analysis enabled us to link populations to their potential growth strategies; however, the differences in metabolic potential observed between the recovered MAGs and total communities suggested that genetic potential of the recovered MAGs did not completely elucidate the metabolic potential of the total communities, depending on the abundance of recovered MAGs. Thus, microbial composition and genetic potential should be described with caution and in consideration of all gene content when no

https://doi.org/10.1021/acs.est.1c00802
Environ. Sci. Technol. 2021, 55, 12683−12693

overwhelming majority of the microbial community was binned into near-complete genomes. This study revealed microbial communities in PF to be phylogenetically and functionally distinct from those in the ALs. Genomic analysis showed that the PF was enriched in populations with the ability to degrade plant-derived polysaccharides and grow via fermentation and nitrate/nitrite reduction. In contrast, the populations recovered from the ALs were shown to acquire energy via aerobic respiration. Gene abundances in the metagenomes further demonstrated that microbial communities from the AL had a tendency to contain a higher abundance of genes associated with methane/ammonia oxidation, CSP and TCSs.

■ ASSOCIATED CONTENT

Supporting Information

The Supporting Information is available free of charge at https://pubs.acs.org/doi/10.1021/acs.est.1c00802.

Additional descriptions of the materials and methods, PCA, estimated number of cells per gram of soil, relative abundance of significantly different taxonomy, genome-enabled metabolic potential, normalized abundances of KOs, phylogenetic analysis, sample and sequencing information, chemical composition of the permafrost soils, sequence information for each selected MAG, key metabolic pathways, and potential metabolic pathways (PDF)

■ AUTHOR INFORMATION

Corresponding Author

Tatiana A. Vishnivetskaya − *Center for Environmental Biotechnology, University of Tennessee, Knoxville, Tennessee 37996, United States;* orcid.org/0000-0002-0660-023X; Email: tvishniv@utk.edu

Authors

Xiaofen Wu − *Center for Environmental Biotechnology, University of Tennessee, Knoxville, Tennessee 37996, United States;* orcid.org/0000-0002-2337-0894

Archana Chauhan − *Center for Environmental Biotechnology, University of Tennessee, Knoxville, Tennessee 37996, United States;* Present Address: Department of Zoology, Panjab University, Chandigarh 160014, India

Alice C. Layton − *Center for Environmental Biotechnology, University of Tennessee, Knoxville, Tennessee 37996, United States*

Maggie C. Y. Lau Vetter − *Department of Geosciences, Princeton University, Princeton, New Jersey 08544, United States;* Present Address: Laboratory of Extraterrestrial Ocean Systems, Institute of Deep-Sea Science and Engineering, Chinese Academy of Sciences, Sanya, Hainan, China

Brandon T. Stackhouse − *Department of Geosciences, Princeton University, Princeton, New Jersey 08544, United States*

Daniel E. Williams − *Center for Environmental Biotechnology, University of Tennessee, Knoxville, Tennessee 37996, United States*

Lyle Whyte − *Department of Natural Resource Sciences, McGill University, Ste. Anne de Bellevue, Quebec H9X 3V9, Canada*

Susan M. Pfiffner − *Center for Environmental Biotechnology, University of Tennessee, Knoxville, Tennessee 37996, United States*

Tullis C. Onstott − *Department of Geosciences, Princeton University, Princeton, New Jersey 08544, United States*

Complete contact information is available at: https://pubs.acs.org/10.1021/acs.est.1c00802

Notes

The authors declare no competing financial interest.

■ ACKNOWLEDGMENTS

This research was funded by the U.S. Department of Energy, Office of Science, Office of Biological and Environmental Research, Genomic Science Program under award number DE-SC0004902. The bioinformatic analyses were supported by the National Science Foundation DEB-1442262 and by the U.S. Department of Energy, Office of Science, Office of Biological and Environmental Research, Genomic Science Program DE-SC0020369.

■ REFERENCES

(1) Tarnocai, C.; Canadell, J. G.; Schuur, E. A. G.; Kuhry, P.; Mazhitova, G.; Zimov, S. Soil Organic Carbon Pools in the Northern Circumpolar Permafrost Region. *Global Biogeochem. Cycles* **2009**, *23*, GB2023.

(2) Schuur, E. A. G.; Abbott, B. Climate Change: High Risk of Permafrost Thaw. *Nature* **2011**, *480*, 32−33.

(3) Melillo, J. M.; Steudler, P. A.; Aber, J. D.; Newkirk, K.; Lux, H.; Bowles, F. P.; Catricala, C.; Magill, A.; Ahrens, T.; Morrisseau, S. Soil Warming and Carbon-Cycle Feedbacks to the Climate System. *Science* **2002**, *298*, 2173−2176.

(4) Cox, P. M.; Betts, R. A.; Jones, C. D.; Spall, S. A.; Totterdell, I. J. Acceleration of Global Warming Due to Carbon-Cycle Feedbacks in a Coupled Climate Model. *Nature* **2000**, *408*, 184−187.

(5) Schuur, E. A. G.; Vogel, J. G.; Crummer, K. G.; Lee, H.; Sickman, J. O.; Osterkamp, T. E. The Effect of Permafrost Thaw on Old Carbon Release and Net Carbon Exchange from Tundra. *Nature* **2009**, *459*, 556−559.

(6) Davidson, E. A.; Janssens, I. A. Temperature Sensitivity of Soil Carbon Decomposition and Feedbacks to Climate Change. *Nature* **2006**, *440*, 165−173.

(7) Hugelius, G.; Strauss, J.; Zubrzycki, S.; Harden, J. W.; Schuur, E. A. G.; Ping, C. L.; Schirrmeister, L.; Grosse, G.; Michaelson, G. J.; Koven, C. D.; O'Donnell, J. A.; Elberling, B.; Mishra, U.; Camill, P.; Yu, Z.; Palmtag, J.; Kuhry, P. Improved Estimates Show Large Circumpolar Stocks of Permafrost Carbon While Quantifying Substantial Uncertainty Ranges and Identifying Remaining Data Gaps. *Biogeosciences Discuss.* **2014**, *11*, 4771−4822.

(8) Peterson, K. M. Plants in Arctic Environments. In *Ecology and the Environment, The Plant Sciences*; Springer: New York, 2014; pp 363−388.

(9) Tedrow, J. C. F.; Cantlon, J. E. Concepts of Soil Formation and Classification in Arctic Regions. *Arctic* **1958**, *11*, 166−179.

(10) Paré, M.; Bedard-Haughn, A. Surface Soil Organic Matter Qualities of Three Distinct Canadian Arctic Sites. *Arctic, Antarct. Alp. Res.* **2013**, *45*, 88−98.

(11) Starr, G.; Oberbauer, S. F.; Ahlquist, L. E. The Photosynthetic Response of Alaskan Tundra Plants to Increased Season Length and Soil Warming. *Arctic, Antarct. Alp. Res.* **2008**, *40*, 181−191.

(12) Singh, B. K.; Bardgett, R. D.; Smith, P.; Reay, D. S. Microorganisms and Climate Change: Terrestrial Feedbacks and Mitigation Options. *Nat. Rev. Microbiol.* **2010**, *8*, 779−790.

(13) Graham, D. E.; Wallenstein, M. D.; Vishnivetskaya, T. A.; Waldrop, M. P.; Phelps, T. J.; Pfiffner, S. M.; Onstott, T. C.; Whyte, L. G.; Rivkina, E. M.; Gilichinsky, D. A.; Elias, D. A.; MacKelprang, R.;

Verberkmoes, N. C.; Hettich, R. L.; Wagner, D.; Wullschleger, S. D.; Jansson, J. K. Microbes in Thawing Permafrost: The Unknown Variable in the Climate Change Equation. *ISME J.* **2012**, *6*, 709−712.
(14) Mackelprang, R.; Waldrop, M. P.; Deangelis, K. M.; David, M. M.; Chavarria, K. L.; Blazewicz, S. J.; Rubin, E. M.; Jansson, J. K. Metagenomic Analysis of a Permafrost Microbial Community Reveals a Rapid Response to Thaw. *Nature* **2011**, *480*, 368−371.
(15) Tveit, A.; Schwacke, R.; Svenning, M. M.; Urich, T. Organic Carbon Transformations in High-Arctic Peat Soils: Key Functions and Microorganisms. *ISME J.* **2013**, *7*, 299−311.
(16) Yergeau, E.; Hogues, H.; Whyte, L. G.; Greer, C. W. The Functional Potential of High Arctic Permafrost Revealed by Metagenomic Sequencing, qPCR and Microarray Analyses. *ISME J.* **2010**, *4*, 1206−1214.
(17) Berendsen, R. L.; Pieterse, C. M. J.; Bakker, P. A. H. M. The Rhizosphere Microbiome and Plant Health. *Trends Plant Sci.* **2012**, *17*, 478−486.
(18) Lau, M. C. Y.; Stackhouse, B. T.; Layton, A. C.; Chauhan, A.; Vishnivetskaya, T. A.; Chourey, K.; Ronholm, J.; Mykytczuk, N. C. S.; Bennett, P. C.; Lamarche-Gagnon, G.; Burton, N.; Pollard, W. H.; Omelon, C. R.; Medvigy, D. M.; Hettich, R. L.; Pfiffner, S. M.; Whyte, L. G.; Onstott, T. C. An Active Atmospheric Methane Sink in High Arctic Mineral Cryosols. *ISME J.* **2015**, *9*, 1880−1891.
(19) Stackhouse, B. T.; Vishnivetskaya, T. A.; Layton, A.; Chauhan, A.; Pfiffner, S.; Mykytczuk, N. C.; Sanders, R.; Whyte, L. G.; Hedin, L.; Saad, N.; Myneni, S.; Onstott, T. C. Effects of Simulated Spring Thaw of Permafrost from Mineral Cryosol on CO_2 Emissions and Atmospheric CH_4 Uptake. *J. Geophys. Res. G Biogeosciences* **2015**, *120*, 1764−1784.
(20) Wagner, D.; Lipski, A.; Embacher, A.; Gattinger, A. Methane Fluxes in Permafrost Habitats of the Lena Delta: Effects of Microbial Community Structure and Organic Matter Quality. *Environ. Microbiol.* **2005**, *7*, 1582−1592.
(21) Coolen, M. J. L.; Orsi, W. D. The Transcriptional Response of Microbial Communities in Thawing Alaskan Permafrost Soils. *Front. Microbiol.* **2015**, *6*, 197.
(22) Vishnivetskaya, T. A.; Layton, A. C.; Lau, M. C. Y.; Chauhan, A.; Cheng, K. R.; Meyers, A. J.; Murphy, J. R.; Rogers, A. W.; Saarunya, G. S.; Williams, D. E.; Pfiffner, S. M.; Biggerstaff, J. P.; Stackhouse, B. T.; Phelps, T. J.; Whyte, L.; Sayler, G. S.; Onstott, T. C. Commercial DNA Extraction Kits Impact Observed Microbial Community Composition in Permafrost Samples. *FEMS Microbiol. Ecol.* **2014**, *87*, 217−230.
(23) Klappenbach, J. A.; Dunbar, J. M.; Schmidt, T. M. rRNA Operon Copy Number Reflects Ecological Strategies of Bacteria. *Appl. Environ. Microbiol.* **2000**, *66*, 1328−1333.
(24) Bouvier, T.; Del Giorgio, P. A. Factors Influencing the Detection of Bacterial Cells Using Fluorescence in Situ Hybridization (FISH): A Quantitative Review of Published Reports. *FEMS Microbiol. Ecol.* **2003**, *44*, 3−15.
(25) Hazen, T. C.; Rocha, A. M.; Techtmann, S. M. Advances in Monitoring Environmental Microbes. *Curr. Opin. Biotechnol.* **2013**, *24*, 526−533.
(26) Bruins, M. R.; Kapil, S.; Oehme, F. W. Microbial Resistance to Metals in the Environment. *Ecotoxicol Env. Saf.* **2000**, *45*, 198−207.
(27) Edgar, R. C. UNOISE2 Improved Error-Correction for Illumina 16S and ITS Amplicon Sequencing. *bioRxiv* **2016**, 081257 DOI: 10.1101/081257.
(28) Wolter, J.; Lantuit, H.; Wetterich, S.; Rethemeyer, J.; Fritz, M. Climatic, Geomorphologic and Hydrologic Perturbations as Drivers for Mid- to Late Holocene Development of Ice-Wedge Polygons in the Western Canadian Arctic. *Permafr. Periglac. Process.* **2018**, *29*, 164−181.
(29) Parks, D. H.; Rinke, C.; Chuvochina, M.; Chaumeil, P.-A.; Woodcroft, B. J.; Evans, P. N.; Hugenholtz, P.; Tyson, G. W. Recovery of Nearly 8,000 Metagenome-Assembled Genomes Substantially Expands the Tree of Life. *Nat. Microbiol.* **2017**, *2*, 1533−1542.
(30) Yuan, C.; Lei, J.; Cole, J.; Sun, Y. Reconstructing 16S rRNA Genes in Metagenomic Data. *Bioinformatics* **2015**, *31*, i35−i43.
(31) Hugenholtz, P.; Skarshewski, A.; Parks, D. H. Genome-Based Microbial Taxonomy Coming of Age. *Cold Spring Harbor Perspect. Biol.* **2016**, *8*, a018085.
(32) Parks, D. H.; Chuvochina, M.; Waite, D. W.; Rinke, C.; Skarshewski, A.; Chaumeil, P. A.; Hugenholtz, P. A Standardized Bacterial Taxonomy Based on Genome Phylogeny Substantially Revises the Tree of Life. *Nat. Biotechnol.* **2018**, *36*, 996−1004.
(33) Parks, D. H.; Chuvochina, M.; Chaumeil, P.-A.; Rinke, C.; Mussig, A. J.; Hugenholtz, P. A Complete Domain-to-Species Taxonomy for Bacteria and Archaea. *Nat. Biotechnol.* **2020**, *38*, 1079−1086.
(34) Chen, Y.-L.; Deng, Y.; Ding, J.-Z.; Hu, H.-W.; Xu, T.-L.; Li, F.; Yang, G.-B.; Yang, Y.-H. Distinct Microbial Communities in the Active and Permafrost Layers on the Tibetan Plateau. *Mol. Ecol.* **2017**, *26*, 6608−6620.
(35) Hultman, J.; Waldrop, M. P.; Mackelprang, R.; David, M. M.; McFarland, J.; Blazewicz, S. J.; Harden, J.; Turetsky, M. R.; McGuire, A. D.; Shah, M. B.; VerBerkmoes, N. C.; Lee, L. H.; Mavrommatis, K.; Jansson, J. K. Multi-Omics of Permafrost, Active Layer and Thermokarst Bog Soil Microbiomes. *Nature* **2015**, *521*, 208−212.
(36) Sun, E. W.-H.; Hajirezaie, S.; Dooner, M.; Vishnivetskaya, T. A.; Layton, A.; Chauhan, A.; Pfiffner, S. M.; Whyte, L. G.; Onstott, T. C.; Lau, M. C. Y. Thaumarchaea Genome Sequences from a High Arctic Active Layer. *Microbiol. Resour. Announc.* **2020**, *9*, No. e00326-20.
(37) Coolen, M. J. L.; van de Giessen, J.; Zhu, E. Y.; Wuchter, C. Bioavailability of Soil Organic Matter and Microbial Community Dynamics upon Permafrost Thaw. *Environ. Microbiol.* **2011**, *13*, 2299−2314.
(38) Lauber, C. L.; Hamady, M.; Knight, R.; Fierer, N. Pyrosequencing-Based Assessment of Soil pH as a Predictor of Soil Bacterial Community Structure at the Continental Scale. *Appl. Environ. Microbiol.* **2009**, *75*, 5111−5120.
(39) Fierer, N.; Leff, J. W.; Adams, B. J.; Nielsen, U. N.; Bates, S. T.; Lauber, C. L.; Owens, S.; Gilbert, J. A.; Wall, D. H.; Caporaso, J. G. Cross-Biome Metagenomic Analyses of Soil Microbial Communities and Their Functional Attributes. *Proc. Natl. Acad. Sci. U.S.A.* **2012**, *109*, 21390−21395.
(40) Sheremet, A.; Jones, G. M.; Jarett, J.; Bowers, R. M.; Bedard, I.; Culham, C.; Eloe-Fadrosh, E. A.; Ivanova, N.; Malmstrom, R. R.; Grasby, S. E.; Woyke, T.; Dunfield, P. F. Ecological and Genomic Analyses of Candidate Phylum WPS-2 Bacteria in an Unvegetated Soil. *Environ. Microbiol.* **2020**, *22*, 3143−3157.
(41) Tian, R.; Ning, D.; He, Z.; Zhang, P.; Spencer, S. J.; Gao, S.; Shi, W.; Wu, L.; Zhang, Y.; Yang, Y.; Adams, B. G.; Rocha, A. M.; Detienne, B. L.; Lowe, K. A.; Joyner, D. C.; Klingeman, D. M.; Arkin, A. P.; Fields, M. W.; Hazen, T. C.; Stahl, D. A.; Alm, E. J.; Zhou, J. Small and Mighty: Adaptation of Superphylum Patescibacteria to Groundwater Environment Drives Their Genome Simplicity. *Microbiome* **2020**, *8*, 51.
(42) Nguyen, S. T. C.; Freund, H. L.; Kasanjian, J.; Berlemont, R. Function, Distribution, and Annotation of Characterized Cellulases, Xylanases, and Chitinases from CAZy. *Appl. Microbiol. Biotechnol.* **2018**, *102*, 1629−1637.
(43) Woodcroft, B. J.; Singleton, C. M.; Boyd, J. A.; Evans, P. N.; Emerson, J. B.; Zayed, A. A. F.; Hoelzle, R. D.; Lamberton, T. O.; McCalley, C. K.; Hodgkins, S. B.; Wilson, R. M.; Purvine, S. O.; Nicora, C. D.; Li, C.; Frolking, S.; Chanton, J. P.; Crill, P. M.; Saleska, S. R.; Rich, V. I.; Tyson, G. W. Genome-Centric View of Carbon Processing in Thawing Permafrost. *Nature* **2018**, *560*, 49−54.
(44) Lipson, D. A.; Haggerty, J. M.; Srinivas, A.; Raab, T. K.; Sathe, S.; Dinsdale, E. A. Metagenomic Insights into Anaerobic Metabolism along an Arctic Peat Soil Profile. *PLoS One* **2013**, *8*, No. e64659.
(45) Rusley, C.; Onstott, T. C.; Vishnivetskaya, T. A.; Layton, A.; Chauhan, A.; Pfiffner, S. M.; Whyte, L. G.; Lau, M. C. Y. Metagenome-Assembled Genome of USCα AHI, a Potential High-

Affinity Methanotroph from Axel Heiberg Island, Canadian High Arctic. *Microbiol. Resour. Announce.* **2019**, *8*, No. e01178-19.
(46) Mondav, R.; Woodcroft, B. J.; Kim, E. H.; Mccalley, C. K.; Hodgkins, S. B.; Crill, P. M.; Chanton, J.; Hurst, G. B.; Verberkmoes, N. C.; Saleska, S. R.; Hugenholtz, P.; Rich, V. I.; Tyson, G. W. Discovery of a Novel Methanogen Prevalent in Thawing Permafrost. *Nat. Commun.* **2014**, *5*, 1−7.
(47) Altshuler, I.; Ronholm, J.; Layton, A.; Onstott, T. C.; Greer, C. W.; Whyte, L. G. Denitrifiers Nitrogen-Fixing Bacteria and N_2O Soil Gas Flux in High Arctic Ice-Wedge Polygon Cryosols. *FEMS Microbiol. Ecol.* **2019**, *95*, fiz049.
(48) Chauhan, A.; Layton, A. C.; Vishnivetskaya, T. A.; Williams, D.; Pfiffner, S. M.; Rekepalli, B.; Stackhouse, B.; Lau, M. C. Y.; Phelps, T. J.; Mykytczuk, N.; Ronholm, J.; Whyte, L.; Onstott, T. C.; Sayler, G. S. Metagenomes from Thawing Low-Soil-Organic-Carbon Mineral Cryosols and Permafrost of the Canadian High Arctic. *Genome Announc.* **2014**, *2*, No. e01217-14.
(49) Grimm, F.; Franz, B.; Dahl, C. (2008) Thiosulfate and Sulfur Oxidation in Purple Sulfur Bacteria, Chapter 9, Dahl, C., Friedrich, C.G. (eds). In *Microbial Sulfur Metabolism*. Springer: Berlin, Heidelberg
(50) Sakurai, H.; Ogawa, T.; Shiga, M.; Inoue, K. Inorganic Sulfur Oxidizing System in Green Sulfur Bacteria. *Photosynth. Res.* **2010**, *104*, 163−176.
(51) Gregersen, L. H.; Bryant, D. A.; Frigaard, N. U. Mechanisms and Evolution of Oxidative Sulfur Metabolism in Green Sulfur Bacteria. *Front. Microbiol.* **2011**, *2*, 116.
(52) Sousa, F. L.; Alves, R. J.; Ribeiro, M. A.; Pereira-Leal, J. B.; Teixeira, M.; Pereira, M. M. The Superfamily of Heme-Copper Oxygen Reductases: Types and Evolutionary Considerations. *Biochim. Biophys. Acta - Bioenerg.* **2012**, *1817*, 629−637.
(53) Morris, R. L.; Schmidt, T. M. Shallow Breathing: Bacterial Life at Low O_2. *Nat. Rev. Microbiol.* **2013**, *11*, 205−212.
(54) Borisov, V. B.; Gennis, R. B.; Hemp, J.; Verkhovsky, M. I. The Cytochrome bd Respiratory Oxygen Reductases. *Biochim. Biophys. Acta, Bioenerg.* **2011**, *1807*, 1398−1413.
(55) Xue, Y.; Jonassen, I.; Øvreås, L.; Taş, N. Metagenome-Assembled Genome Distribution and Key Functionality Highlight Importance of Aerobic Metabolism in Svalbard Permafrost. *FEMS Microbiol. Ecol.* **2020**, *96*, 1−13.
(56) Guo, X.; Yin, H.; Cong, J.; Dai, Z.; Liang, Y.; Liu, X. RubisCO Gene Clusters Found in a Metagenome Microarray from Acid Mine Drainage. *Appl. Environ. Microbiol.* **2013**, *79*, 2019−2026.
(57) Jaffe, A. L.; Castelle, C. J.; Dupont, C. L.; Banfield, J. F. Lateral Gene Transfer Shapes the Distribution of RuBisCO among Candidate Phyla Radiation Bacteria and DPANN Archaea. *Mol. Biol. Evol.* **2019**, *36*, 435−446.
(58) Carter, M. S.; Zhang, X.; Huang, H.; Bouvier, J. T.; Francisco, B. S.; Vetting, M. W.; Al-Obaidi, N.; Bonanno, J. B.; Ghosh, A.; Zallot, R. G.; Andersen, H. M.; Almo, S. C.; Gerlt, J. A. Functional Assignment of Multiple Catabolic Pathways for D-Apiose Article. *Nat. Chem. Biol.* **2018**, *14*, 696−705.
(59) Tabita, F. R.; Hanson, T. E.; Li, H.; Satagopan, S.; Singh, J.; Chan, S. Function, Structure, and Evolution of the RubisCO-Like Proteins and Their RubisCO Homologs. *Microbiol. Mol. Biol. Rev.* **2007**, *71*, 576−599.
(60) Hügler, M.; Sievert, S. M. Beyond the Calvin Cycle: Autotrophic Carbon Fixation in the Ocean. *Annu. Rev. Mar. Sci.* **2011**, *3*, 261−289.
(61) Yin, W.; Wang, Y.; Liu, L.; He, J. Biofilms: The Microbial "Protective Clothing" in Extreme Environments. *Int. J. Mol. Sci.* **2019**, *20*, 3423.
(62) Mackelprang, R.; Saleska, S. R.; Jacobsen, C. S.; Jansson, J. K.; Taş, N. Permafrost Meta-Omics and Climate Change. *Annu. Rev. Earth Planet Sci.* **2016**, *44*, 439−462.
(63) Stock, A. M.; Robinson, V. L.; Goudreau, P. N. Two-Component Signal Transduction. *Annu. Rev. Biochem.* **2000**, *69*, 183−215.
(64) Feng, L.; Chen, S.; Hu, Y. PhoPR Positively Regulates WhiB3 Expression in Response to Low pH in Pathogenic Mycobacteria. *J. Bacteriol.* **2018**, *200*, No. e00766-17.
(65) Laub, M. T. (2010) The Role of Two-Component Signal Transduction Systems in Bacterial Stress Responses, Chapter 4. G. Storz and R. Hengge, (eds). In *Bacterial Stress Responses*
(66) Freeman, Z. N.; Dorus, S.; Waterfield, N. R. The KdpD/KdpE Two-Component System: Integrating K^+ Homeostasis and Virulence. *PLoS Pathog.* **2013**, *9*, No. e1003201.
(67) Baek, J. H.; Lee, S. Y. Transcriptome Analysis of Phosphate Starvation Response in Escherichia Coli. *J. Microbiol. Biotechnol.* **2007**, *17*, 244−252.
(68) Cai, S. J.; Inouye, M. EnvZ-OmpR Interaction and Osmoregulation in Escherichia Coli. *J. Biol. Chem.* **2002**, *277*, 24155−24161.
(69) Cybulski, L. E.; Albanesi, D.; Mansilla, M. C.; Altabe, S.; Aguilar, P. S.; De Mendoza, D. Mechanism of Membrane Fluidity Optimization: Isothermal Control of the Bacillus Subtilis Acyl-Lipid Desaturase. *Mol. Microbiol.* **2002**, *45*, 1379−1388.

https://doi.org/10.1021/acs.est.1c00802
Environ. Sci. Technol. 2021, 55, 12683−12693